ON WEIGHTED ORTHOGONAL BASIS FUNCTION IN MLS WITH MESHLESS LOCAL PETROV GALERKIN METHOD

Rituraj Singh* and Roman Trobec

"Jožef Stefan" Institute, Parallel and Distributed Systems Laboratory, Jamova cesta 39, 1000 Ljubljana, Slovenia.

* Corresponding author's email: Rituraj.Singh@ijs.si

doi: https://doi.org/10.21467/proceedings.100.11

ABSTRACT

The moving least square scheme is among the most successful schemes to generate meshfree shape functions in meshfree methods. It is computationally expensive due to computation of the inverse of the moment matrix. Recently, a weighted orthogonal basis function based moving least square approximation has been used in few meshfree methods such as element free Galerkin method, boundary element free method and global boundary node method. The moment matrix becomes diagonal matrix due to the orthogonal basis functions, and thus, the moment matrix becomes diagonal with trivial inverse. In the current work, weighted orthogonal basis functions based moving least square approximation is used in meshless local Petrov Galerkin method. We have tested this new method with the meshless local Petrov Galerkin method for one- and two-dimensional Poisson equation. The numerical experiments have confirmed that the new approach provides the same accuracy and convergence rate but with higher computational efficiency than the classical moving least square with meshless local Petrov Galerkin method.

1. Introduction

In most of the meshfree methods, moving least square (MLS) scheme is used to generate meshfree shape functions. The MLS scheme has some drawbacks, i.e. devoid of the Kronecker delta property, instability at higher grid resolution, and computational complexity due to inversion of the moment matrix. Devoid of Kronecker delta property makes it difficult to impose essential boundary conditions (EBCs), and, methods such as penalty approach or Lagrange multiplier are required to impose EBCs. This makes the method more complicated and time consuming. To resolve this problem, recently, interpolating moving least square method and improved interpolating moving least square schemes have been proposed. These variants of the MLS have Kronecker delta property and EBCs can be easily applied on boundaries. In the interpolating MLS, a singular weight function is used, and new basis functions, based on MLS basis functions, are developed [1]. The use of a singular weight function in the interpolating MLS put some limitations. To overcome this problem improved interpolating MLS scheme was proposed [2]. Both versions of the MLS have been used in some meshfree methods such as EFG, boundary element free method (BEFM), and global boundary node method (GBNM) [2]–[5].

The MLS scheme becomes unstable at higher grid resolutions because the moment matrix becomes ill-conditioned. This problem was solved by using shifted and scaled polynomials basis functions in the MLS and its variants. Li and his co-workers [3], [6] have studied the variation of condition number with respect to grid size in both MLS and interpolating MLS in GBNM. The condition number of the moment matrix becomes independent of the grid size.

Proceedings DOI: 10.21467/proceedings.100; Series: AIJR Proceedings; ISSN: 2582-3922; ISBN: 978-81-942709-6-6 (eBook)

Another variant of MLS is based on weighted orthogonal basis functions. In this paper, we give an acronym of this new MLS as OMLS. In this scheme, weighted orthogonal basis functions are generated based on MLS basis functions. The moment matrix in the OMLS becomes a diagonal matrix, and thus, inversion of the moment matrix can be neglected. This saves significantly the CPU time. However, this scheme does not possess Kronecker delta property. Liew et al. proposed BEFM based on OMLS for two-dimension elasto-dynamics and elasticity problems [7], [8]. Zhang et al. applied OMLS in the EFG method for different problems such as elasto-dynamics, wave equation, potential problem, and heat conduction problems [9]–[15]. Wang and Sun presented OMLS for regularized long wave equation [16]. Li et al. presented an error analysis of OMLS [17] and they implemented OMLS in the GBNM [18]. Wang et al. used OMLS in the lattice Boltzmann method in place of the MLS scheme for fluid-solid interaction problem [19]. Cheng et al. solved space fractional wave equations by using OMLS [20].

In the current work, weighted orthogonal basis function based moving least square approximation (OMLS) is used in meshless local Petrov Galerkin method (OMLPG). We have tested OMLS for surface and curve fittings, then, the OMLPG method has been used to solve Poisson equation in one- and two-dimensions. We briefly describe the derivation of MLS and OMLS in the next section followed by MLPG formulation and numerical results.

2. Approximation Schemes

In this section we first give a mathematical derivation of the moving least square (MLS) scheme, then, a method for generation of OMLS basis functions is presented.

2.1 Moving Least Square Scheme (MLS)

Let **x** be an evaluation point at which the shape functions and derivatives are to be computed. MLS approximation can be written as

$$u^h(\mathbf{x}) = \sum_{j=1}^{m} p_j(\mathbf{x}) a_j(\mathbf{x}) = \mathbf{p}^{\mathrm{T}}(\mathbf{x})\mathbf{a}(\mathbf{x}) \tag{1}$$

where $\mathbf{p}^T(\mathbf{x})$ is a row vector containing m number of basis functions. For example, in 2-D space, the quadratic basis is given as

$$\mathbf{p}^T(\mathbf{x}) = \left[1,\ x_1, x_2, x_1^2,\ x_1 x_2,\ x_2^2\right], \tag{2}$$

where $m=6$ is a number of basis functions. The coefficient vector **a(x)** is determined by minimizing a weighted discrete L_2 norm

$$\begin{aligned} J &= \sum_{i=1}^{ns} w(\mathbf{x}, \mathbf{x}_i)[u^h(\mathbf{x}, \mathbf{x}_i) - u(\mathbf{x}_i)]^2 \\ &= \sum_{i=1}^{ns} w(\mathbf{x}, \mathbf{x}_i)[\mathbf{p}^{\mathbf{T}}(\mathbf{x}_i)\mathbf{a}(\mathbf{x}) - u(\mathbf{x}_i)]^2 \end{aligned} \tag{3}$$

ISBN: 978-81-942709-6-6 ISSN: 2582-3922

where $w(\mathbf{x},\mathbf{x}_i)$ is a weight function, *ns* is the number of nodes in the support domain, and $u(\mathbf{x}_i)$ is the nodal parameter of the field variable at node $\mathbf{x}_i$. Above equation can be written in the matrix form

$$\mathbf{A}(\mathbf{x})\mathbf{a}(\mathbf{x}) = \mathbf{B}(\mathbf{x})\mathbf{u} \tag{4}$$

where

$$\mathbf{A}(\mathbf{x}) = \sum_{i=1}^{ns} w(\mathbf{x},\mathbf{x}_i)\mathbf{p}(\mathbf{x}_i)\mathbf{p}^{\mathrm{T}}(\mathbf{x}_i) \tag{5}$$

$$\mathbf{a}(\mathbf{x}) = [a_1(\mathbf{x}), a_2(\mathbf{x}), \ldots\ldots\ldots, a_m(\mathbf{x})]^{\mathrm{T}} \tag{6}$$

$$\mathbf{B}(\mathbf{x}) = \sum_{i=1}^{ns} w(\mathbf{x},\mathbf{x}_i)\mathbf{p}(\mathbf{x}_i)$$

$$\mathbf{u} = [\bar{u}_1, \bar{u}_2, \ldots \bar{u}_{ns}]^T$$

The MLS approximation is re-written as

$$u^h(\mathbf{x}) = \sum_{i=1}^{ns} \Phi_i u_i = \mathbf{\Phi}^T(\mathbf{x})\mathbf{u}, \tag{7}$$

where and $\mathbf{\Phi}$ is the meshless shape function given by

$$\Phi_i(\mathbf{x}) = \sum_{j=1}^{m} p_j(\mathbf{x})(\mathbf{A}^{-1}(\mathbf{x})\mathbf{B}(\mathbf{x}))_{ji} = \mathbf{p}^{\mathbf{T}}\mathbf{A}^{-1}\mathbf{B} \tag{8}$$

In the current work, we have chosen quartic weight function

$$w(\mathbf{x}-\mathbf{x}_i) = \begin{cases} 1-6d^2+8d^3-3d^4 & \text{if } 0 \le d \le 1 \\ 0 & \text{if } d > 1 \end{cases}, \quad d = \frac{\|\mathbf{x}-\mathbf{x}_i\|}{r_w} \tag{9}$$

r_w is the radius of the weighted domain in which weight function is non-zero.

2.2 MLS based on Orthogonal Basis Functions (OMLS)

Definition of new basis function is given below which are orthogonal

$$\tilde{p}_i(\mathbf{x}) = p_i(\mathbf{x}) - \sum_{k=1}^{i-1} \frac{(p_i, \tilde{p}_k)}{(\tilde{p}_k, \tilde{p}_k)} \tilde{p}_k, \quad i = 1,2,3... \tag{10}$$

where $\tilde{p}_i(\mathbf{x})$ is the new orthogonal basis function of the OMLS scheme, $p_i(\mathbf{x})$ is basis function of MLS. Let *f* and *g* be functions of **x.** The inner product $(f \cdot g)$ is defined as

$$(f \cdot g)_{\mathbf{x}} = \sum_{k=1}^{ns} w(\mathbf{x}, \mathbf{x}_k) f(\mathbf{x}_k) g(\mathbf{x}_k) \tag{11}$$

New weighted orthogonal basis function can be obtained as

$$\tilde{p}_1(\mathbf{x}) = 1$$

$$\tilde{p}_2(\mathbf{x}) = x_1 - \frac{(p_2, \tilde{p}_1)}{(\tilde{p}_1, \tilde{p}_1)} p_1 = x_1 - \sum_{k=1}^{ns} w(\mathbf{x}, \mathbf{x}_k) x_{1k} \Big/ \sum_{k=1}^{ns} w(\mathbf{x}, \mathbf{x}_k)$$

Similarly, other weighted orthogonal basis functions for OMLS can be obtained. The remaining procedure is the same as of MLS, thus, we are not repeating it here.

The moment matrix **A** is a diagonal matrix as basis functions are weighed orthogonal. The **A** matrix can be written as

$$\mathbf{A}(\mathbf{x}) = \begin{bmatrix} (\tilde{p}_1 \cdot \tilde{p}_1) & 0 & \cdots & 0 \\ 0 & (\tilde{p}_2 \cdot \tilde{p}_2) & \cdots & 0 \\ \vdots & \cdots & \ddots & \vdots \\ 0 & \cdots & & (\tilde{p}_m \cdot \tilde{p}_m) \end{bmatrix}$$

Similar to MLS, the OMLS approximation is written as

$$u^h(\mathbf{x}) = \sum_{i=1}^{ns} \Phi_i u_i = \mathbf{\Phi}^T(\mathbf{x})\mathbf{u}, \tag{12}$$

where and $\mathbf{\Phi}$ is the meshless shape function given by

$$\Phi_i(\mathbf{x}) = \sum_{j=1}^{m} p_j(\mathbf{x})(\mathbf{A}^{-1}(\mathbf{x})\mathbf{B}(\mathbf{x}))_{ji} = \tilde{\mathbf{p}}^{\mathbf{T}} \mathbf{A}^{-1} \mathbf{B}_i \tag{13}$$

We have used a shifted and scaled approach to provide stability at denser grid points [6].

3. MLPG Formulation

The MLPG formulation for the Poisson equation is described below. The equation is solved in the global domain Ω bounded by the boundary Γ [21].

$$\begin{aligned} &\nabla^2 u - p = 0 && \text{in } \Omega \\ &u(\mathbf{x}) = \bar{u}(\mathbf{x}) && \text{for } \mathbf{x} \in \Gamma \end{aligned} \tag{14}$$

$\bar{u}$ is the specified field variable on the boundary Γ. A general weak form for the numerical solution of Eq. (14) can be obtained from the weighted residual statement

ISBN: 978-81-942709-6-6 ISSN: 2582-3922

$$\int_{\Omega_Q} \left[\nabla^2 u - p\right] v \; \mathrm{d}\Omega = 0 \tag{15}$$

where Ω_Q is a local domain and v is the test function. Continuity requirement of the above equation can be reduced by applying divergence theorem, that yields to the weak form given by

$$\int_{\Gamma_Q} u_{,x} n_{,x} v \; \mathrm{d}\Gamma - \int_{\Omega_Q} \left[u_{,x} v_{,x} + pv\right] \mathrm{d}\Omega = 0 \tag{16}$$

where Γ_Q denotes the boundary of the local domain, Ω_Q and shorthand notations have been used. If the test function in the standard MLPG method is the same as the weight function of the MLS approximation, then, it vanishes at the boundary of the local domain. Hence, evaluation of the boundary integral term which is completely inside the global domain is not required. The use of MLPG discretization leads to the system of algebraic equations.

$$\mathbf{Ku} = \mathbf{F}$$

Where **K** is the stiffness matrix, **u** is the vector of unknown nodal parameters, and **F** is the force vector. Elements of stiffness matrix **K** and force vector **F** are as follows:

$$K_{ij} = \begin{cases} \Phi_j(\mathbf{x}_i) & \mathbf{x}_i \in \Gamma \\ \int_{\Gamma_Q} \Phi_{j,x}(\mathbf{x}) n_{,x} v(\mathbf{x}, \mathbf{x}_i) \mathrm{d}\Gamma_Q - \int_{\Omega_Q} \Phi_{j,x}(\mathbf{x}) v_{,x}(\mathbf{x}, \mathbf{x}_i) \mathrm{d}\Omega_Q & \mathbf{x}_i \notin \Gamma \end{cases} \tag{17}$$

$$F_i = \begin{cases} \bar{u}(\mathbf{x}_i) & \mathbf{x}_i \in \Gamma \\ \int_{\Omega_Q} pv(\mathbf{x}, \mathbf{x}_i) d\Omega_Q & \mathbf{x}_i \notin \Gamma \end{cases} \tag{18}$$

The direct interpolation method is used to impose EBCs [22].

4. Numerical Results and Discussion

This section provides numerical results of MLS and OMLS schemes. We have done curve and surface fittings tests in one- and two-dimensions respectively. The C/C++ code have been developed, and, numerical test have been conducted on *intel core i7* processor with serial programming. Then, results for the solution of the Poisson equation, solved by MLPG and OMLS based MLPG (OMLPG), are shown for one- and two-dimensions. In all presented results, we have used quadratic basis and quadratic spline weight function in both approximations. The number of nodes in the support domain of every evaluation point is constant, thus, the radius of the support domain varies accordingly [23]. Absolute error is calculated as

$$\text{Absolute error} = \left|(u_i - u^e{}_i)\right|$$

where u_i and u_i^e are approximate and exact values at node i respectively. Relative percentage error is calculated by l_2 norm

$$\text{Relative \% error} = 100 \times \sqrt{\sum_{i=1}^{N}(u_i - u^e{}_i)^2} \Bigg/ \sqrt{\sum_{i=1}^{N} u^e{}_i{}^2}$$

where N is the total number of points. The radius of the quadrature domain in the MLPG method is calculated as

$$r_q = \alpha_Q d_c$$

In the present case, we have used a uniform grid, and the d_c is grid spacing. The dimensionless parameter of the quadrature domain (α_Q) is set constant equal to 0.9 in the MLPG implementation.

4.1 Curve Fitting in 1-D

In this section results for curve fitting tests in one dimension are shown. The study of convergence and accuracy has done for OMLS and it is compared with MLS approximation for a known trigonometric function.

We evaluate the function approximation at evaluation points using data in grid points. Five evaluation points are distributed between two consecutives grid points in the 1-D domain. The error of approximated known function with reference to the exact value of known function has been calculated on these evaluation points. We have used 6 number of nodes in the support domain (ns = 6). The trigonometric function used is

$$u = \sin^2(2\pi x) + \cos(2\pi x)$$

Approximated known function, its derivatives, and absolute errors obtained by both MLS and OMLS have been shown in Fig. 1 and Fig. 2 respectively. Errors are the same for both approximations. Results are shown for 20 grid points. We also show convergence for both approximations (Fig. 3). The convergence rate is as expected and the same for both approximations. The convergence rate of function's derivative approximation is slightly lower than the convergence of function approximation.

4.2 Surface Fitting in 2-D

Surface fitting tests are done in the two-dimensional unit square domain. Known trigonometric function

$$u = \sin(2\pi x_1)\cos(3\pi x_2)$$

is approximated by MLS and OMLS in both cases with $ns=12$. Evaluation points approximately four times the number of grid points are distributed in the domain. The function is evaluated on these evaluation points using known data in the grid points. The approximation of function converges well by MLS and OMLS, however, similar to 1-D case, the convergence rate of function's derivative approximation is lower Fig. 4.

ISBN: 978-81-942709-6-6 ISSN: 2582-3922

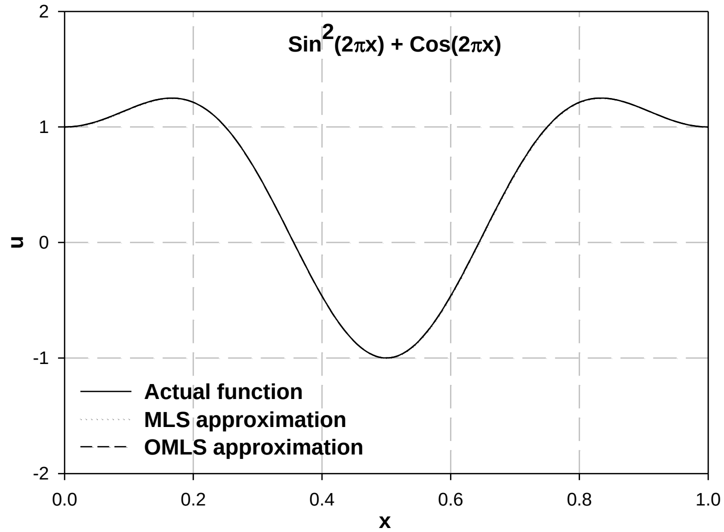

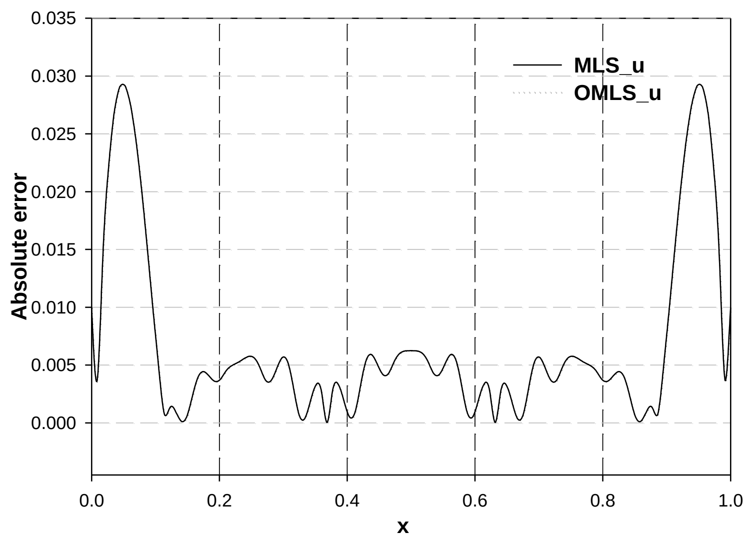

Fig. 1 Approximated functions (above) and absolute errors of 1-D approximation for MLS and OMLS (below).

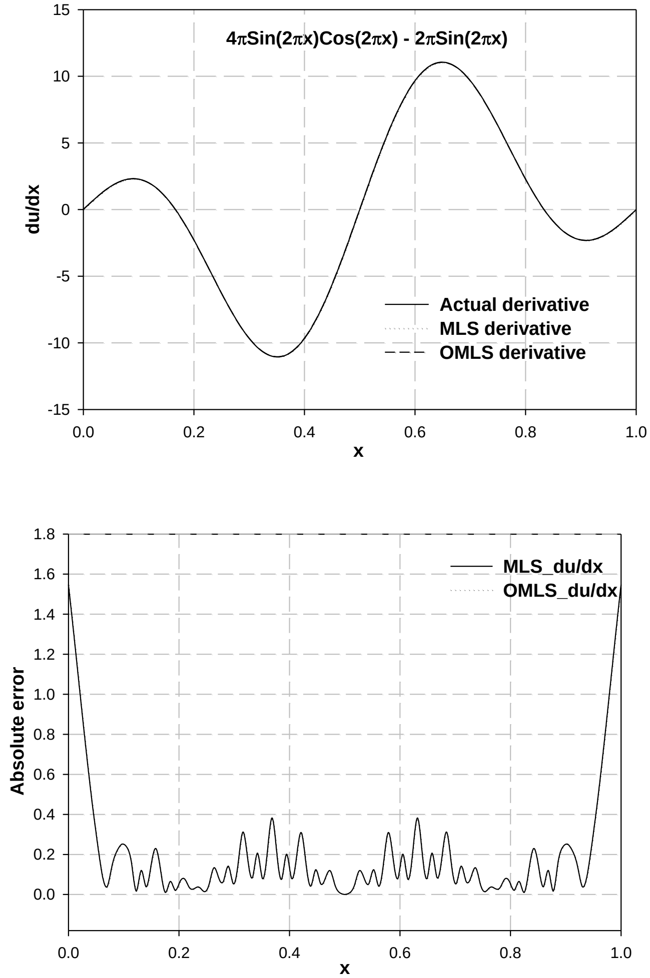

Fig. 2 Approximated function derivatives (above) and absolute errors of 1-D approximation for MLS and OMLS (below).

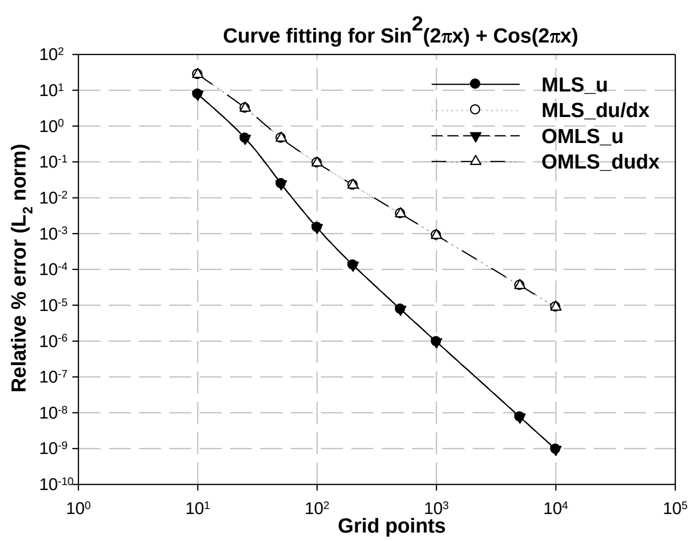

Fig. 3 Convergence of 1-D function approximation and its derivative approximation for MLS and OMLS.

Proceedings DOI: 10.21467/proceedings.100
Series: AIJR Proceedings
ISBN: 978-81-942709-6-6
ISSN: 2582-3922

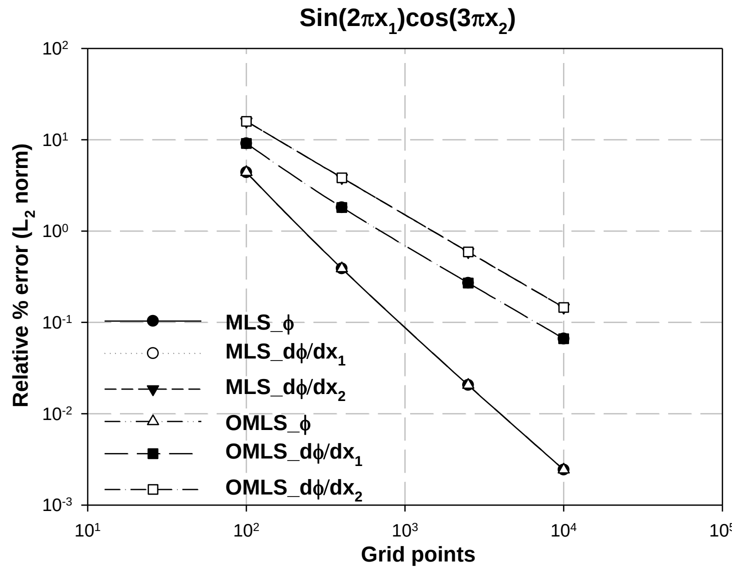

Fig. 4 Convergence of 2-D function approximation and its derivative approximation for MLS and OMLS**.**

4.3 MLPG Results in 1-D

Poisson equation with EBCs is solved by the MLPG method in the one-dimension unity domain.

$$\frac{d^2u}{dx^2} + \kappa = 0 \tag{19}$$

The value of constant (κ) is assumed 2500 and the specified value of field variable is zero at both boundary nodes. The analytical solution can be obtained directly. Fig. 5 shows the exact solution, MLPG, and OMLPG solutions. These results are obtained by using ns = 6, with 8 Gaussian points for numerical integration and 100 grid points. The accuracy of the MLPG method with both approximations is as expected and similar for both methods.

4.4 MLPG Results in 2-D

A Poisson equation is solved by MLPG and OMLPG methods in the unit square domain. There is only EBCs. A field variable is zero on the boundary.

$$\nabla^2 u = -200\pi^2 \sin(\pi x_1)\sin(\pi x_2) \tag{20}$$

An analytical solution is be obtained as

$$u = 100\sin(\pi x_1)\sin(\pi x_2)$$

We use 6×6 Gaussian points in the quadrature domain for numerical integration. The circular test domain is chosen. Errors are calculated on grid points. Fig. 6 shows an OMLPG solution and absolute error, and, we have found the same results for the MLPG method. A convergence of both methods is shown in Fig. 7

Both methods have the same accuracy and convergence rate. Computation time for MLPG and OMLPG has been compared as shown in Fig. 8. CPU time taken by different modules of the code has been shown such as grid generation, searching nodes for support domain, solution of system equations and total time. The OMLPG method has low computational cost while generating shape functions. However, the algorithm for search nodes in for the support domain shows the highest computational complexity. In Table 1, computational efficiency of OMLS with reference to MLS for generating shape functions is shown. The OMLS is approximately 10 % more efficient than MLS.

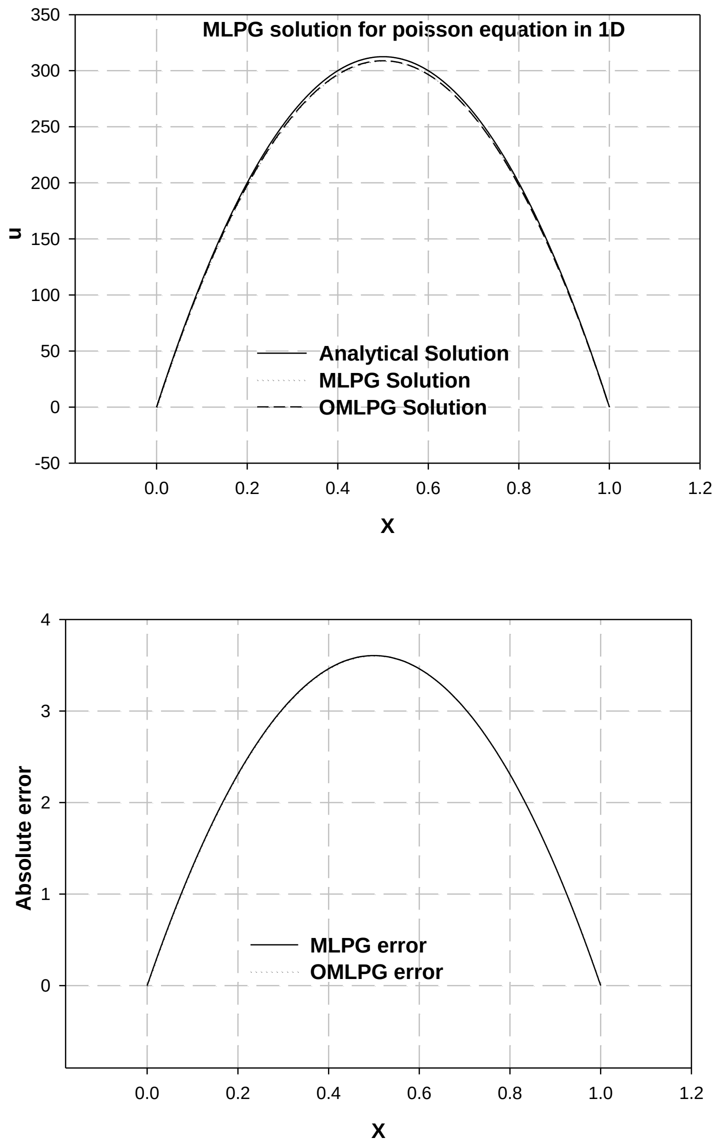

Fig. 5 Comparison of 1-D MLPG solution with different approximation schemes (above) and absolute error (below) .

ISBN: 978-81-942709-6-6 ISSN: 2582-3922

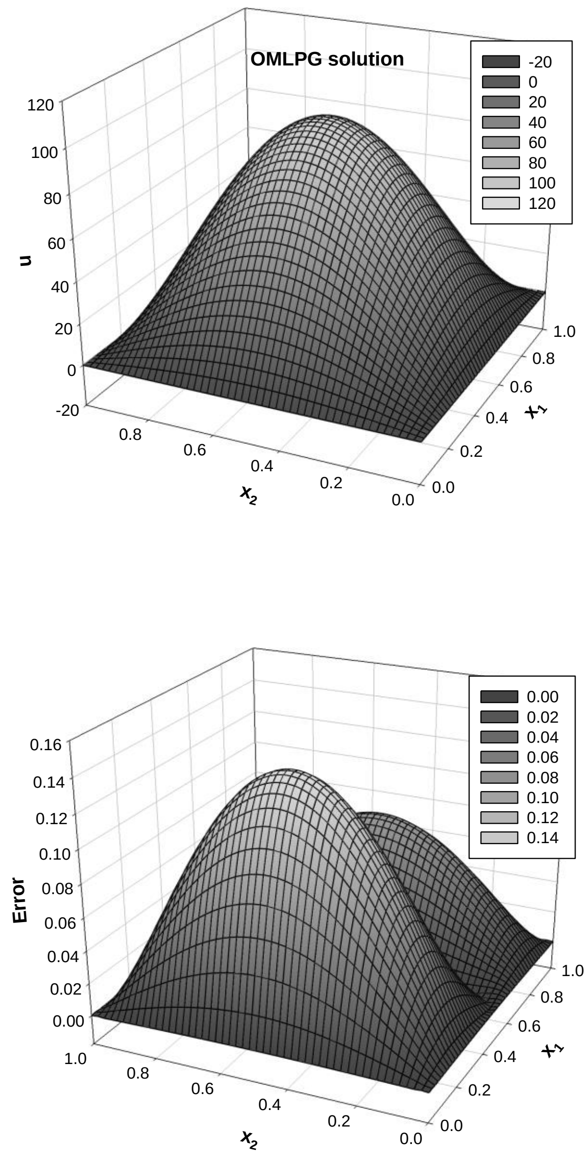

Fig. 6 OMLPG solution in 2D (above) and absolute error (below)

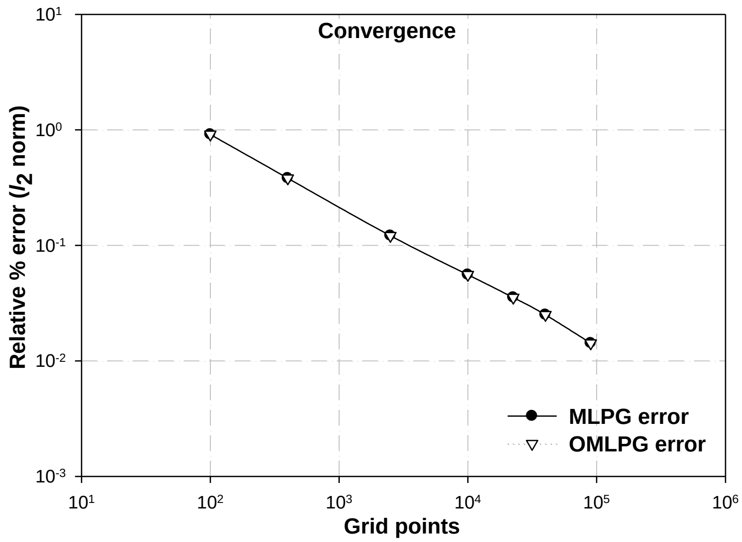

Fig. 7 Convergence of MLPG and OMLPG in 2D.

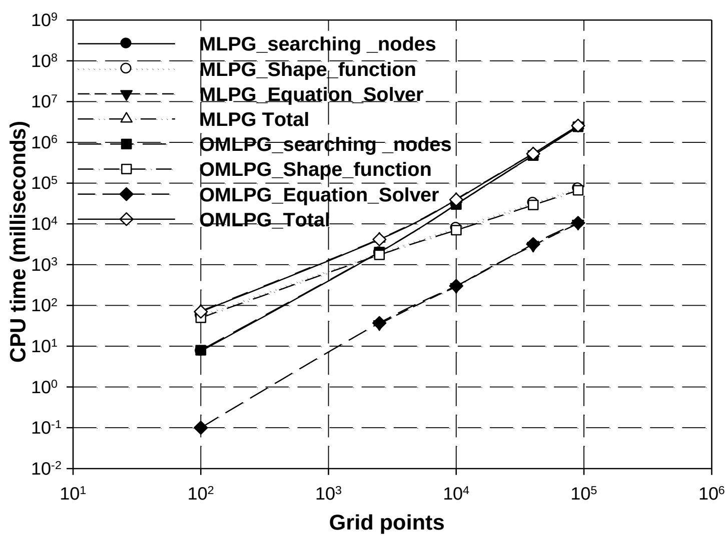

Fig. 8 CPU time comparison of MLPG and OMLPG.

Table 1 Computation time of MLS and OMLS with efficiency of OMLS with reference to MLS.

Grid points	CPU_{MLS} (ms)	CPU_{OMLS} (ms)	$\eta = \frac{100(CPU_{MLS} - CPU_{OMLS})}{CPU_{MLS}}$
100	56.1140	49.8340	11.19
2500	1918.55	1708.59	10.94
10000	7970.7300	7012.3800	12.02
40000	32825.0000	29014.9000	11.60
90000	74181.3000	66266.8000	10.66

5. CONCLUSIONS

The computational cost of MLS based meshfree methods is significant due to the inversion of the moment matrix in the MLS procedure. A new version of MLS has been used with some meshfree methods in which weighted orthogonal basis functions are used. This makes the moment matrix diagonal which eliminates the inversion process. We have implemented OMLS approximation within the MLPG method to observe the performance. The obtained results show that OMLS based MLPG produces the same accuracy and convergence rate as the standard MLS based MLPG, however, at approximately 10% lower computational cost. In further work, we plan to implement the *k-d* tree algorithm to improve the efficiency of searching support domain nodes and we will test the OMLPG method for the solution of time dependent problems.

6. ACKNOWLEDGMENTS

This work was partly supported by the Slovenian Research Agency under Grant P2-0095 “Parallel and Distributed Computing”.

REFERENCES

[1] H. Ren and Y. Cheng, “The interpolating element-free Galerkin (IEFG) method for two-dimensional potential problems,” *Eng. Anal. Bound. Elem.*, vol. 36, no. 5, pp. 873–880, 2012.

[2] J. F. Wang, F. X. Sun, and Y. M. Cheng, “An improved interpolating element-free Galerkin method with a nonsingular weight function for two-dimensional potential problems,” *Chinese Phys. B*, vol. 21, no. 9, p. ID-090204, 2012.

[3] X. Li and Q. Wang, “Analysis of the inherent instability of the interpolating moving least squares method when using improper polynomial bases,” *Eng. Anal. Bound. Elem.*, vol. 73, pp. 21–34, 2016.

[4] F. Li and X. Li, “The interpolating boundary element-free method for unilateral problems arising in variational inequalities,” *Math. Probl. Eng.*, vol. 2014, p. ID-518727, 2014.

[5] X. Li, “A meshless interpolating Galerkin boundary node method for Stokes flows,” *Eng. Anal. Bound. Elem.*, vol. 51, pp. 112–122, 2015.

[6] X. Li and S. Li, “On the stability of the moving least squares approximation and the element-free Galerkin method,” *Comput. Math. with Appl.*, vol. 72, no. 6, pp. 1515–1531, 2016.

[7] K. M. Liew, Y. Cheng, and S. Kitipornchai, “Boundary element-free method (BEFM) for two-dimensional elastodynamic analysis using Laplace transform,” *Int. J. Numer. Methods Eng.*, vol. 64, no. 12, pp. 1610–1627, 2005.

[8] K. M. Liew, Y. Cheng, and S. Kitipornchai, “Boundary element-free method (BEFM) and its application to two-dimensional elasticity problems,” *Int. J. Numer. Methods Eng.*, vol. 65, no. 8, pp. 1310–1332, 2006.

[9] Z. Zhang, K. M. Liew, Y. Cheng, and Y. Y. Lee, “Analyzing 2D fracture problems with the improved element-free Galerkin method,” *Eng. Anal. Bound. Elem.*, vol. 32, no. 3, pp. 241–250, 2008.

[10] Z. Zhang, K. M. Liew, and Y. Cheng, “Coupling of the improved element-free Galerkin and boundary element methods for two-dimensional elasticity problems,” vol. 32, pp. 100–107, 2008.

[11] Z. Zhang, P. Zhao, and K. M. Liew, “Analyzing three-dimensional potential problems with the improved element-free Galerkin method,” *Comput. Mech.*, vol. 44, no. 2, pp. 273–284, 2009.

[12] Z. Zhang, P. Zhao, and K. M. Liew, “Improved element-free Galerkin method for two-dimensional potential problems,” *Eng. Anal. Bound. Elem.*, vol. 33, no. 4, pp. 547–554, 2009.

[13] Z. Zhang, D. M. Li, Y. M. Cheng, and K. M. Liew, “The improved element-free Galerkin method for three-dimensional wave equation,” *Acta Mech. Sin. Xuebao*, vol. 28, no. 3, pp. 808–818, 2012.

[14] Z. Zhang, S. Y. Hao, K. M. Liew, and Y. M. Cheng, "The improved element-free Galerkin method for two-dimensional elastodynamics problems," *Eng. Anal. Bound. Elem.*, vol. 37, no. 12, pp. 1576–1584, 2013.

[15] Z. Zhang, J. Wang, Y. Cheng, and K. M. Liew, "The improved element-free Galerkin method for three-dimensional transient heat conduction problems," *Sci. China Physics, Mech. Astron.*, vol. 56, no. 8, pp. 1568–1580, 2013.

[16] J. Wang and F. Sun, "A meshless method based on the improved interpolating moving least-squares method for the regularized long wave equation," *Appl. Mech. Mater.*, vol. 101–102, pp. 467–470, 2012.

[17] X. Li, H. Chen, and Y. Wang, "Error analysis in Sobolev spaces for the improved moving least-square approximation and the improved element-free Galerkin method," *Appl. Math. Comput.*, vol. 262, pp. 56–78, 2015.

[18] X. Li and S. Zhang, "Meshless analysis and applications of a symmetric improved Galerkin boundary node method using the improved moving least-square approximation," *Appl. Math. Model.*, vol. 40, pp. 2875–2896, 2016.

[19] W. Q. Wang, Y. Yan, and G. R. Liu, "An IB-LBM implementation for fluid-solid interactions with an MLS approximation for implicit coupling," *Appl. Math. Model.*, vol. 62, pp. 638–653, 2018.

[20] R. Cheng, F. Sun, and J. Wang, "Meshless analysis of two-dimensional two-sided space-fractional wave equation based on improved moving least-squares approximation," *Int. J. Comput. Math.*, vol. 95, no. 3, pp. 540–560, 2018.

[21] S. N. Atluri and T. Zhu, "A new meshless local Petrov-Galerkin (MLPG) approach in computational mechanics," *Comput. Mech.*, vol. 22, no. 2, pp. 117–127, 1998.

[22] R. Singh and K. M. Singh, "On preconditioned BiCGSTAB solver for MLPG method applied to heat conduction in complex geometry," *Numer. Heat Transf. Part B Fundam.*, vol. 72, no. 5, pp. 377–391, 2017.

[23] M. Sterk and R. Trobec, "Meshless solution of a diffusion equation with parameter optimization and error analysis," *Eng. Anal. Bound. Elem.*, vol. 32, no. 7, pp. 567–577, 2008.